Computational Approach to Detect Instability and Incipient Motion of Large Riprap Rocks

Cezary Bojanowski[1], Steven Lottes[2]
Transportation Research and Analysis Computing Center
Nuclear Engineering Division,
Argonne National Laboratory
9700 S. Cass Avenue, Argonne, IL 60439-4828, USA
cbojanowski@anl.gov[1], slottes@anl.gov[2]

Abstract

Bridge scour is the process of removal of sediment from around bridge abutments or piers. In the most severe cases, scour leads to failure of bridges. One of the ways to stop or prevent the scour is to reinforce the riverbed by placing large rocks on the portion of the riverbed vulnerable to scour at bridge foundation structures (method called riprap installation). The sizing of riprap in scour countermeasure design is based mostly on limited field observations and scaled laboratory tests under ideal controlled conditions. The actual size of riprap required for many field applications is too large for testing in the laboratory. As a consequence, there is significant uncertainty in the formulas for sizing riprap.

This paper presents a technique to couple computational fluid dynamics and computational structural mechanics programs (STAR-CCM+ and LS-DYNA®) to analyze the interaction of large rocks with the water flow in rivers and predict incipient motion of the riprap rocks. STAR-CCM+ is able to handle free surface flows with millions of computational cells and complex geometries. LS-DYNA is superior in handling collisions of moving objects and contact with boundaries. For these reasons, the external file based coupling of these two programs was concluded to be the best currently available approach to the computational analysis of onset of riprap motion leading to exposure of the shielded riverbed.

The methodology was used to analyze the bridge over the Middle Fork Feather River in northern California. The bathymetry of the river in the vicinity of the bridge was obtained from a sonar scan of the site and used as the geometry of the numerical model. A rock shape was laser scanned to represent realistic riprap rocks. Several coupled simulations have been performed with varying flow conditions to identify failure conditions for the riprap.

Keywords: FSI, code coupling, mesh morphing, remeshing,

Introduction

Local scour at bridge piers is a potential safety hazard and a major concern of transportation agencies. If it is determined that scour at bridge piers can adversely affect the stability of a bridge, scour countermeasures to protect the piers are considered. Riprap installations are one of many countermeasure alternatives to prevent scour and to secure piers against failure [1]. The sizing of riprap rocks is based mostly on limited field observations and scaled laboratory tests under ideal, controlled conditions. The size of riprap required for many field applications is too large for testing in any laboratory. As a consequence, there is significant uncertainty in the formulas for sizing riprap [2]. Current design methodologies and scour evaluation procedures do not provide a clear means to analyze when the rocks might become displaced under flood conditions and, hence, further advanced computational mechanics techniques are required to assess the rock stability and, thereby, ascertain the scour vulnerability of the bridge.

From the computational mechanics point of view, the analysis of riprap stability can be considered a Fluid Structure Interaction (FSI) problem. Historically, computational fluid dynamics (CFD) software used for

solving fluid flows and computational structural mechanics (CSM) software used for solving the deformations and stresses in solid bodies were developing independently. In recent years a number of CFD and CSM software vendors have been developing the capabilities needed to solve FSI problems within an integrated software package. In many cases these vendors are recognized leaders in the field of either CFD or CSM, but not necessarily in both of them, and integrated FSI software, if available, is not yet capable of handling, with sufficient accuracy, large problems with complex geometries and interactions such as riprap onset of motion in a river environment. Until industry proven FSI solvers are available, coupling highly robust and reliable CFD and CSM software through the development of data exchange and concurrent control coupling procedures appears to be the best approach to solving these complex, engineering FSI problems. In this work, SIEMENS's STAR-CCM+ [3] CFD software and LSTC's LS-DYNA CSM software were used to develop coupling procedures for the detailed analysis of the onset of motion of riprap rocks.

Tracking incipient motion of riprap rocks in a real life application faces several problems. The most important one of them is the complexity of the geometry of the riverbed surrounding the affected piers. The riprap installation usually has hundreds of rocks placed in a semi-organized manner in several layers. Representing all the rocks in the model is nearly impossible, however, sufficient engineering accuracy may be obtained with a reasonable approximation of the armor bed geometry. The second problem pertains to the extent of the domain that has to be considered in the CFD model for proper analysis of flood conditions. The upstream boundary of the computational domain needs to be far enough away from the zone of interest so that the velocity profile can develop by the time the flow reaches the area of the bridge. In the varied bathymetry of a real river bed the variations constantly perturb the velocity profile. In most cases placing the upstream boundary about ten river hydraulic diameters upstream is sufficient. The downstream outlet boundary needs to be placed far enough downstream so that no recirculation zones created by flow obstructions, like piers, are crossing the outflow boundary. In that case the recirculation zone may pull fluid into the domain through the outlet boundary violating the boundary conditions and the computation normally diverges. The outlet boundary should also be far enough downstream so that conditions there do not influence the upstream zone of interest. Placing the outflow boundary about ten river hydraulic diameters downstream of the last obstruction is usually sufficient.

The third issue is a proper handling of the changes in the geometry of the CFD model. STAR-CCM+ is capable of solving flow problems in domains containing many solid objects in relative motion along arbitrary paths through the fluid domain. Mesh motion and mesh morphing (adaptation through mesh stretching) techniques were implemented in it for handling arbitrary motions of objects. These features allow for deforming the computational mesh due to moving boundaries. However, large displacements of the rocks, as well as, collisions between the riprap rocks, may cause the stretched cells to lose sufficient cell quality for accurate solution of the governing equations, or the algorithm may collapse some cells and cause negative volume cell termination of the computation. The feature that is still not present in STAR-CCM+ is an automatic interaction between morphing and remeshing of the domain in case cell quality becomes too poor.

The presence of abovementioned issues makes it nearly impossible to solve the FSI problem for onset of riprap motion in either LS-DYNA (including ICFD, MM-ALE, and SPH) or STAR-CCM+ alone. Thus, the primary objectives of this work were:

(1) Develop an efficient and automatic procedure for file-based data exchange between STAR-CCM+ and LS-DYNA for the purpose of FSI modeling and in particular tracking the incipient motion of large riprap rocks in the river flow,
(2) Develop java macros for controlling STAR-CCM+ to automatically handle updating of the geometry and the mesh of the model based on rock motion data from LS-DYNA,
(3) Establish the validity of the procedure through a simulation of lab-controlled case, and
(4) Apply the developed coupling procedure to analyze the riprap installed at the Middle Fork Feather River Bridge.

Methodologies for Coupling Software

In general, there are two groups of coupling solutions for FSI problems: monolithic and partitioned [4]. The monolithic approach involves solving the coupled set of equations for the fluid and structural domains as a single problem. Although this approach may seem the most natural one, it can be more difficult to adjust solver parameters to obtain a converged solution than with the partitioned approach. Additionally, complex geometries and large displacements pose another challenge that is hard to overcome using this method. The use of robust CFD and CSM software from vendors who specialize in those areas naturally leads to using a partitioned approach where the equations are solved iteratively one domain at a time and coupling conditions (equality of displacements and stresses on common interfaces) are set via file-based data exchange from the solution of the other domain.

In riprap FSI analysis the motion of a rock results in an evolving position and orientation that substantially changes the pressure distribution over the surface of the rock, requiring two-way coupling for this problem. Two-way coupling can be either weak or strong. Weak coupling is presented in Figure 1.2a. In a weakly (or loosely) coupled step *n,* the solution in the fluid region, including the pressure and shear stress distribution, is found on the movable riprap rock surface boundaries at the start of a time step obtained from the structural solver from the previous step, *n-1*. This pressure and stress distribution is subsequently passed to the structural solver, which will yield a solution giving the solid boundary displacement and velocity that is passed to the CFD solver for use in time step *n+1*. The structural solver may require smaller time steps than the fluid solver if effects like contact, such as a rock colliding with surrounding rocks on the bed, are taken into account. Thus the fluid solver time step may be different than structural solver time step, however, the sum of time steps computed on both the structural and fluid domains between data exchange must be equal and that sum establishes the coupling time step. The number of steps and length of time steps is determined by the complexity of the physics modeled in each solver. The selection of the leading part in that scheme, CSM or CFD, is made by the user. Due to the fact that there are no inner iterations in that coupling step, this method is also known as an explicit type of coupling.

Figure 1.2 b presents a schematic of the strong coupling procedure. In this scheme the two problems are also numerically decoupled. However, within each time step *n,* the CFD and CSM solvers exchange interface conditions computed by the separate solvers during the iteration to converge the time step. An updated location of the structure's boundary in the structural step is fed to the CFD model and a new pressure field is found. Instead of progressing to the next step, the updated pressures are used one more time to find a different state of the structure within the same time step in the inner iteration *m+1*. Usually these new positions are averaged together with the positions obtained in the previous inner iteration *m* to improve stability of the method. Due to the presence of the inner iterations in that scheme it is also called an implicit coupling method. It usually leads to more accurate results but causes a linear increase of the computational cost with the number of inner iterations. For problems where an oscillatory type of motion is not the primary response of the structure, good results can be obtained with the use of an explicit coupling scheme with an appropriately adjusted coupling time step.

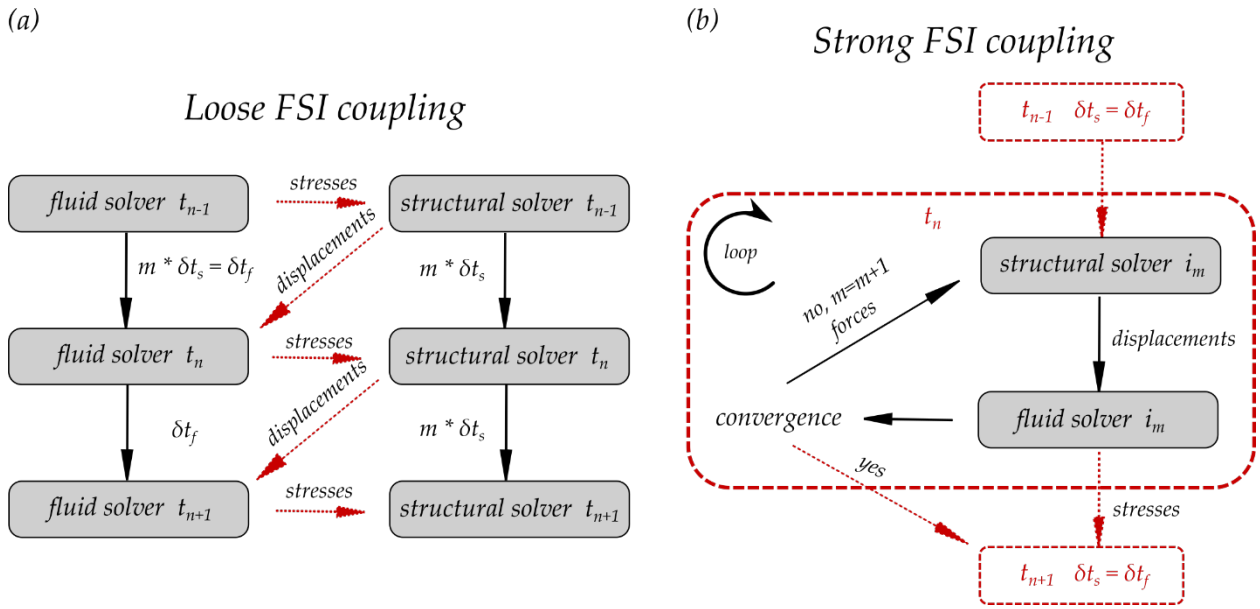

Figure 1.1: Loose and strong FSI coupling schemes

Workflow of the File Based Data Exchange with Explicit Coupling

The implemented explicit coupling involves two separate solvers: STAR-CCM+ [3] performing CFD calculations and LS-DYNA [5], [6] performing structural analysis. The analysis is split into two sub problems. STAR-CCM+ calculates the flow field and resulting pressure and shear stress distribution on rocks, while LS-DYNA calculates the motion of rocks due to the pressure and shear stresses exerted by the fluid on the rock surface and the effects of contact forces. A new position of a rock after the coupling step is subsequently imported into STAR-CCM+ as a basis for the next time step calculation. Because the rocks are treated as rigid bodies, and their behavior is far from regular harmonic motion, an explicit coupling procedure is sufficient to obtain first order accuracy in the solution of the rock motion. The small time step required in LS-DYNA to handle body interactions and in STAR-CCM+ to keep the mesh morphing stable was assumed to be sufficient to compute the onset of rock motion and the trajectory to adequate engineering accuracy.

Figure 1.3 presents the workflow of the procedure to analyze incipient motion of riprap for a given arrangement and flow velocity. The procedure is executed in a LINUX environment with a control program written in the Python language. The program starts execution of needed components of LS-DYNA and STAR-CCM+, including the solvers and meshing software, and LS-PrePost® (LS-DYNA pre- and post-processing software). It also translates output files into a neutral NASTRAN format recognized by both software packages. The analysis procedure begins with initialization runs in both solvers started manually. The LS-DYNA run provides the initial position of the rocks under gravity loading in a drop simulation. This position is used as a basis for CFD domain geometry. The CFD model is run until pseudo steady state conditions are achieved with all rocks stationary. Subsequently the Python program is started with the scheme in which the STAR-CCM+ simulation leads the coupling step. Execution of the CFD part requires a Java macro to run STAR-CCM+, to import rock displacements, and to map them from the CSM mesh to the CFD mesh and vice versa. It is almost always the case that the resolution between the fluid and structural grids is different, especially when two separate solvers are handling the fluid and solid domains. STAR-CCM+ provides accurate data mappers for non-conforming meshes [3]. This mapping has to be performed at each time step as the underlying mesh deforms. The effect of mesh morphing as a consequence of body motion is presented in Figure 1.4. The displacements of the body are distributed throughout the morphed fluid domain to maintain cell quality. No cells are added or removed in the morphing process and their neighbor relationships are preserved so the mesh topology remains constant. The Arbitrary Lagrangian-Eulerian (ALE) algorithm is invoked to solve transport

equations resulting from the moving underlying mesh [3]. It allows for retaining the exact shape of the interface between the solid and the fluid.

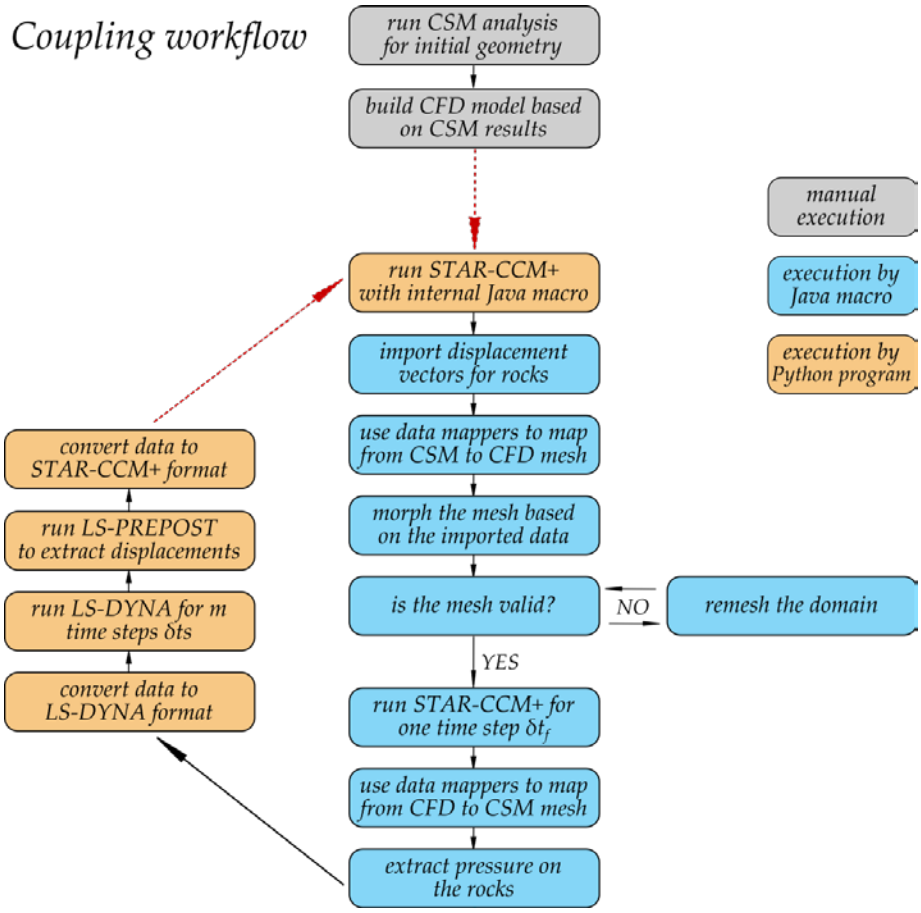

Figure 1.2: Current implementation of coupling workflow between STAR-CCM+ and LS-DYNA

Most of the effort in developing the FSI coupling went into resolving moving and morphing mesh problems that arise when rock motion collapses the space between a rock and another solid surface and problems that arose in the mapping and data exchange between the CFD and CSM software. The resolution of these problems yielded coupling software for data mapping, data exchange, and automated mesh morphing failure recovery that makes it possible to carry out the analysis without frequent intervention of the user.

The mesh morpher uses a sophisticated algorithm that yields a high-quality mesh in the whole computational domain based on the initial mesh and the displacement of the boundaries. However, in cases where the displacement of a rock becomes large or it comes in contact with a solid boundary, the cells may become too distorted and of such poor quality that the solver diverges. As mentioned earlier, a remeshing procedure is not yet integrated with morphing and requires external intervention. In such cases the Java macro executes a remeshing of the whole domain. A cross section of remeshed domain after failure of the mesh morpher is shown in Figure 1.4. The time step of calculations is selected such that full domain remeshing is avoided in the initial steps.

Once a CFD time step δt_f is converged, the pressure and shear stresses on movable rock surfaces are mapped from the CFD mesh on the rocks to the CSM mesh and exported to file. The Java macro as well as the STAR-CCM+ solver are stopped. Next an LS-DYNA simulation is performed for m shorter time steps, δt_s, such that $m\ \delta t_s = \delta t_f$, the length of the coupling step. The resulting displacement vectors from LS-DYNA are extracted and translated to NASTRAN format so that they can be imported into STAR-CCM+ for the next step. After this, the whole loop is repeated until termination time.

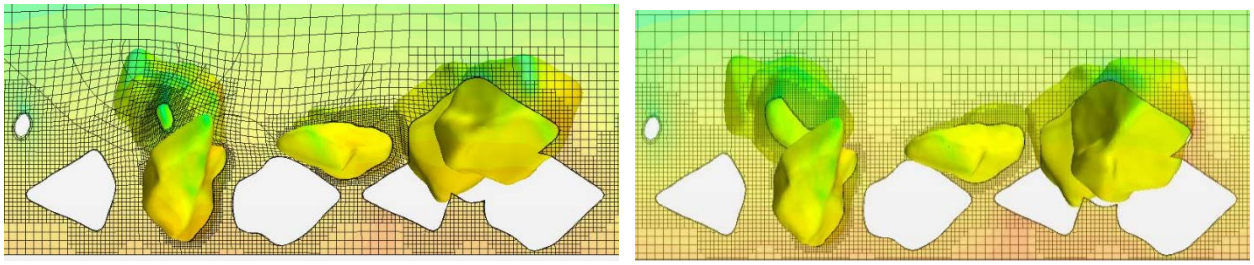

Figure 1.3: Mesh distortion as a result of morphing (right) Remeshed domain after failure of the mesh morpher

Application of the FSI Coupling for Analysis of the Middle Fork Feather River Bridge Riprap Installation

One of locations where the riprap was used to mitigate worsening flood conditions near piers is the Middle Fork Feather River Bridge. It is located on State Route 89 in Plumas County, California near the towns of Blairsden and Graeagle. The bridge was built in 1955 and the river channel was realigned at the time to straighten the flow upstream of the bridge. In 1988 during high winter flows the channel avulsed from the path of the channel after the realignment project toward the path at the time the bridge was built. As a result, the flow now enters the bridge at a strong angle and causes excessive backwater and deep scour at one of the piers (Pier-3). The aerial view of the current condition together with a sketch of the historic channel alignment and the 1955 realignment are shown in Figure 2.1. As an aftermath, the bridge was determined to be scour critical based on the resulting combination of vertical contraction scour and the local pier scour. To mitigate this scour critical condition, a rock mattress consisting of 1 Ton rock over filter fabric was placed around one of the piers in 2011. However, the design of the rock mattress did not consider the increase in flow velocity under the structure caused by the flow separation below the superstructure from the vertical contraction of the flow [7].

Model Development

The riverbed geometry model was constructed based on the 2011 bathymetry survey and GPS coordinates of the area around the bridge [7], [8]. The bed surface was subdivided into the river bed and land portions so different roughness coefficients could be used for each of these boundaries in the CFD model (see Figure 2.2). Additionally, an area surrounding the pier was bounded with a box where denser mesh could be used for more accurate results.

The point cloud bathymetry was numerically enhanced using MeshLab [9] and triangulated to obtain a raw surface used as a base for the CFD mesh. The covered domain was approximately 285 m long, 120 m wide and about 7 m high. The boundary types used in the model are also shown in Figure 2.2. Due to problems with enforcing pressure boundaries on the outlet, where large recirculation zones were developing, the domain was extended by another 300 m. There was no detailed data regarding the profile of the river in that region so the extension was built based on the last cross section of the surveyed domain with a slope of 0.3%.

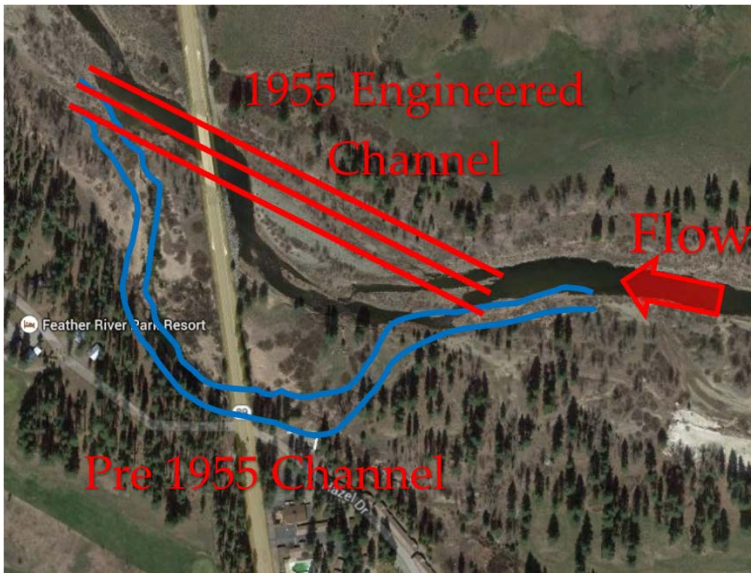

Figure 2.1: Historic, realigned and current river channel alignment [10]; Map data ©2018 Google

Figure 2.3 shows surface mesh of the bed after the rocks have been placed near the affected pier. The subregion in vicinity of the Pier-3 was separated from the rest of the domain. Internal interfaces were placed on the boundaries of that region that were in contact with the outer, global region. In the pure CFD analysis the entire domain together with the extensions was used. However, to simplify the FSI computations, only this sub region was used. The analyzed time in FSI computations was short (several seconds) as compared to the CFD analysis (several minutes). The water flow around the pier doesn't change in such short period of time. Thus, FSI analysis on the extracted subregion with appropriate boundary conditions copied from the interfaces used in CFD was considered to be equivalent to the global domain analysis. This approach not only reduces the computational time required by the model, through the reduction of the cell count but also removes the requirement to use multi-phase physics for water-air interface reconstruction. Analysis of the subdomain uses the so called closed lid (single phase) simulation in which the entire analyzed subdomain is submerged under water. Figure 2.3 shows the cross section through the volume mesh in the global model. The section marked with purple color is the subregion used in the FSI. The subregion contained approximately 2.2M cells, while the global model had nearly 4.1M cells.

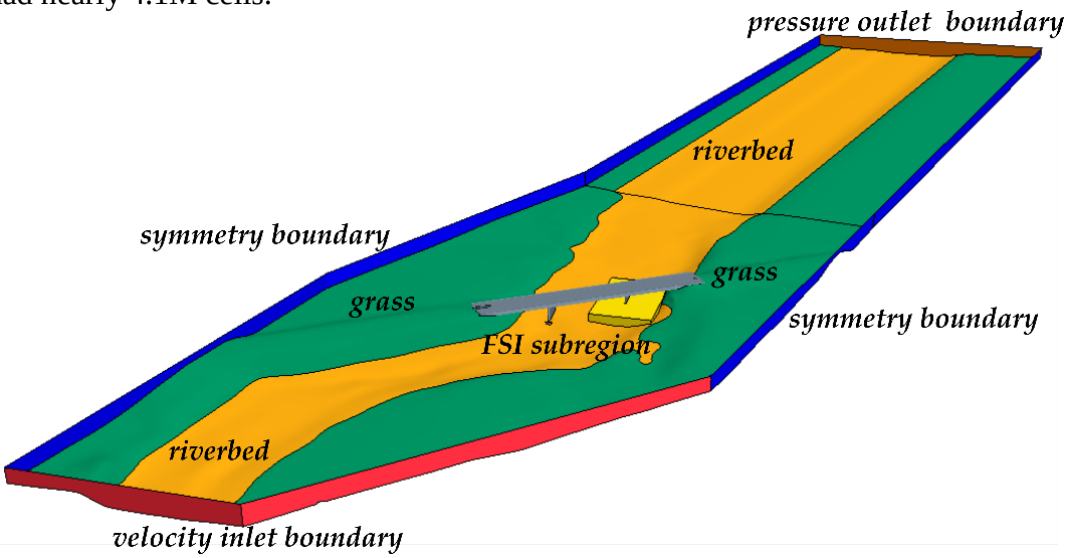

Figure 2.2: Definition of the boundaries in the CFD model

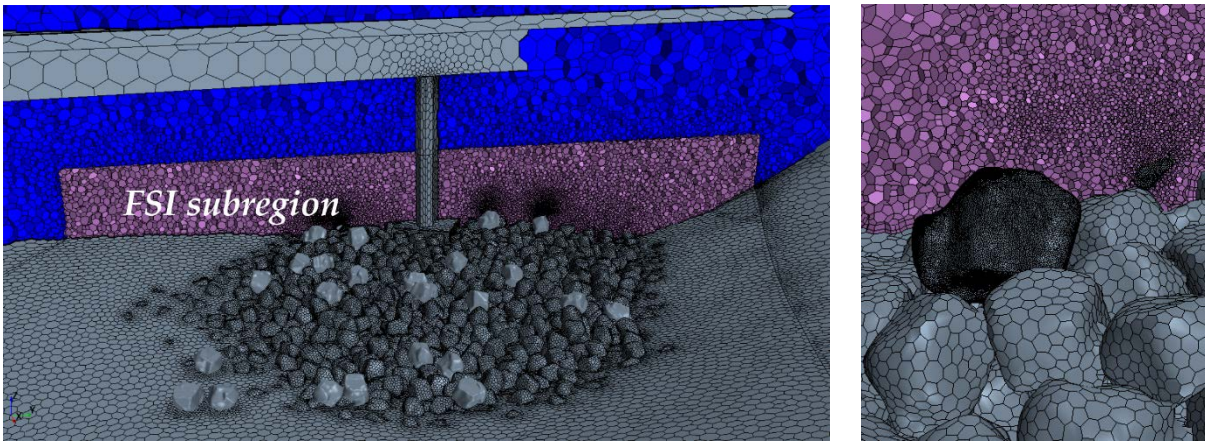

Figure 2.3: Cross section through the finite volume mesh used in STAR-CCM+ model

Over 2,500 rocks were included in the CFD model used for the FSI analysis. They were placed in the scour hole semi-manually, meaning smaller clusters of rocks were copied and changed slightly to introduce some variation in their shape and layout. The geometry of the rocks suffers from several simplifications regarding the precise shape and distribution of the rocks. To minimize these effects, the Turner-Fairbank Highway Research Center (TFHRC) ordered another, more detailed investigation of the installed riprap using sonar techniques. Together with the pictures of the riprap taken during low flows they sought to complement the numerical modeling and improve its accuracy (See Figure 2.4 and Figure 2.5).

Figure 2.4: Pictures of riprap installation near Pier-3 during and after the construction

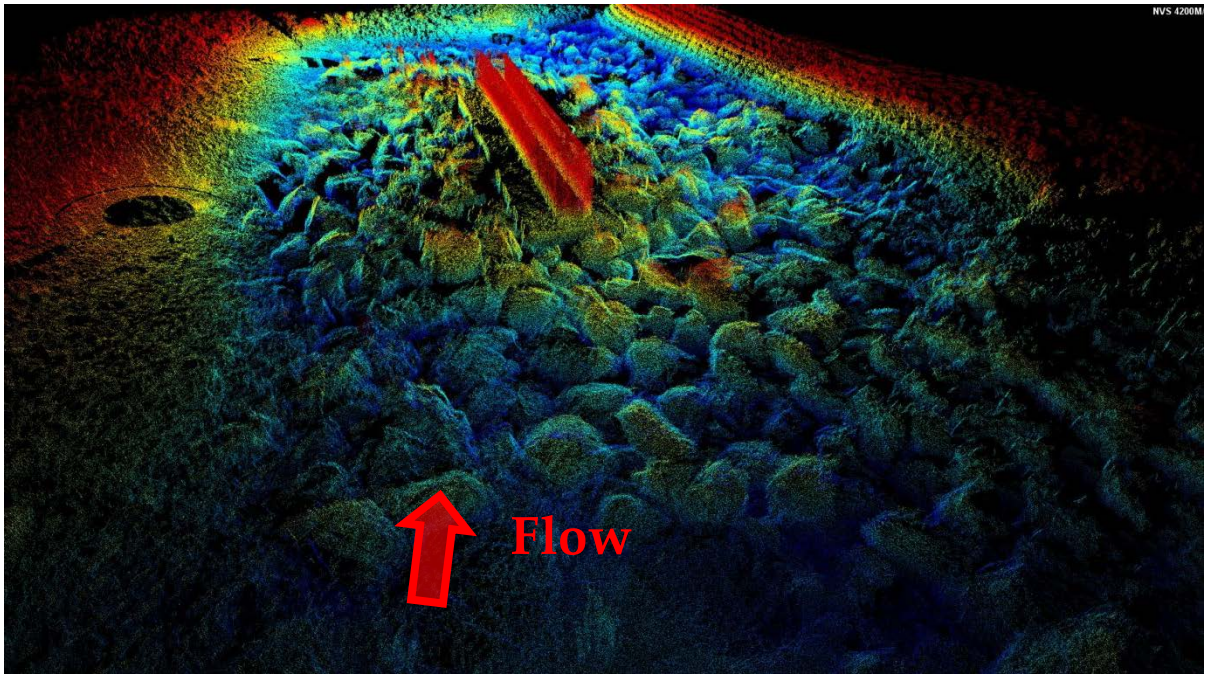

Figure 2.5: Front view on the pier with installed riprap from a sonar scan

The sonars are not physically able to scan voids between the rocks precisely because most of them are out of the equipment view lines. The geometries created based on these limited scans would reduce to a minimum the flow between the rocks by closing voids in the rock layers that do not show up in scans. Thus, the primary use of these scans was to define the overall geometry of the riprap installation and estimate the correct size of the rocks. The scans allowed for identifying the precise extent of the riprap and slopes on each side of the pier. The shape of the new embankment was also easily identifiable. Figure 2.5 shows a point cloud of the scanned bed by one of the sonar techniques.

The photographs taken at the site together with the sonar scans indicated that many of the rocks could be smaller than 1T rocks. For that reason, it was assumed that in the FSI simulation 40 moveable rocks with different sizes would be included: ten 1T rocks, ten 0.8T rocks, ten 0.6T rocks, and ten 0.4T rocks.

The moveable rocks were placed sparsely covering the riprap zone shown by colored rocks in Figure 2.6. The placement of the movable rocks could not be performed manually. They had to be dropped in LS-DYNA and their equilibrium positions had to be found via a finite element (FE) simulation. That way before the FSI simulation is started, they had proper contact with their neighbors and they didn't move any more if forces other than gravity weren't present in the system. The LS-DYNA model was comprised of over a million shell elements and 40 inertia elements attached to the center of gravity (CG) of the moveable rocks. The bed used in LS-DYNA was constructed from the wrapped surface obtained by exporting the STAR-CCM+ boundary mesh. Explicit time integration was used with a time step of 4.50E-06 sec.

Figure 2.6 shows the vicinity of pier-3 together with moveable rocks in their final positions after the drop simulation (pre-FSI). The 0.4 T rocks are highlighted with orange color, 0.6 T rocks are green, 0.8 T rocks are red, and 1.0 T rocks are blue. Some of the moveable rocks are sticking slightly above the neighboring non-moveable rocks. The 0.4 Ton rocks in the front of the riprap are entirely exposed to the flow. This is another factor contributing to conservatism in the computed results.

Results and Analysis

From the initial CFD analysis, hydrodynamic forces on all moveable rocks were extracted in a local coordinate system that was aligned with the Pier-3 and the flow under the bridge. Figure 2.6 shows the rocks with highest forces as found in the CFD simulation of a 100-year flood event. The three most critical rocks in each weight category are labeled. Most of the critical rocks are located west from the pier closer to the center of the bridge opening, where the average velocity was the highest. Table 2.1 shows all the force components on these twelve most vulnerable rocks. The highest Y components of the forces reached about 2.5 kN, and highest Z components reached about 5.5 kN. Although these are the rocks with the highest forces acting on them, the final outcome of FSI suggests that some other rocks may move first. Their interaction with other rocks is the crucial and in many cases the deciding factor with respect to their stability in the riprap installation. From this analysis it appears that the most vulnerable in overall are the smallest rocks, as expected. The ratio between their weight and the resultant force acting on them is the highest.

In order to perform the FSI analysis, the problem was further simplified, as mentioned earlier. Only the vicinity closest to the pier with highest scour risk was used in the FSI. Velocity fields on the outer boundaries of the FSI subdomain were applied based on the global analysis. Average inlet velocity on the frontal face for that case was around 3.4 m/s (11.1 ft/s) for a 100-year flood.

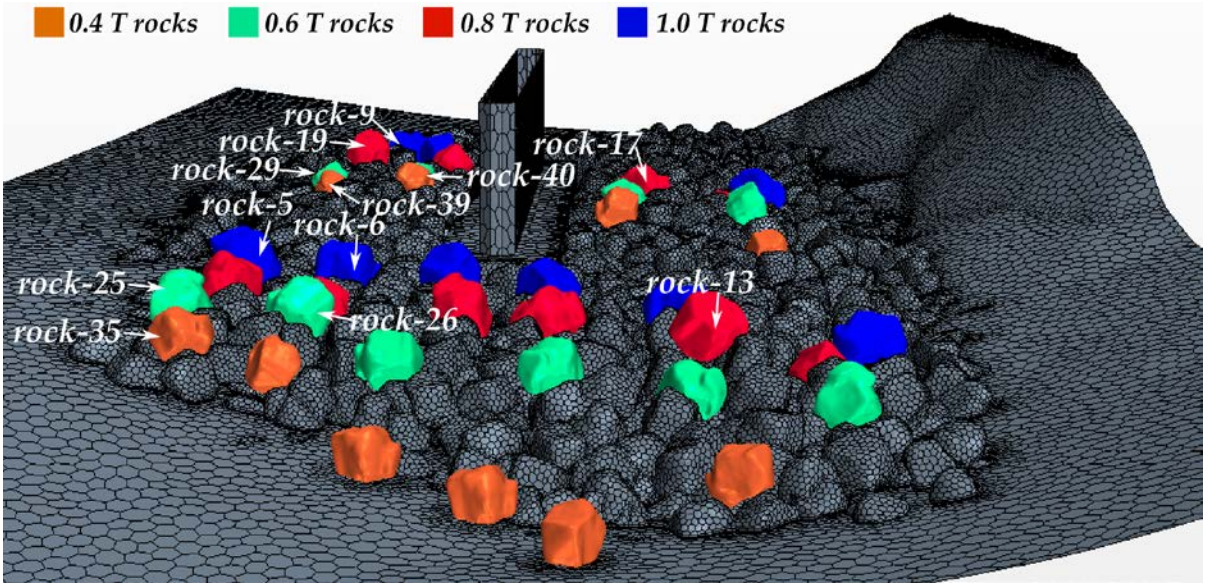

Figure 2.6: Location of the rocks with the highest forces in CFD analysis

Table 2.1: Forces on the critical rocks in the simulation with discharge of 30,100 cfs (100 year flood)

Rock #	X Force	Y Force	Z Force	Resultant	Ratio to weight
1 Ton (9.81 kN)					
6	-0.06	1.68	5.50	5.75	0.59
5	-0.87	2.45	5.10	5.72	0.58
9	-1.31	1.45	5.15	5.51	0.56
0.8 Ton (7.85 kN)					
19	-0.15	2.50	5.35	5.91	0.75
17	-0.40	1.70	3.70	4.09	0.52
13	0.09	1.10	3.75	3.91	0.50
0.6 Ton (5.88 kN)					
25	-0.95	1.32	3.45	3.81	0.65
29	-0.24	1.06	3.55	3.71	0.63
26	-0.38	1.08	3.45	3.64	0.62
0.4 ton (3.92 kN)					
35	0.43	1.25	2.80	3.10	0.79
39	0.10	0.80	2.65	2.77	0.71
40	0.10	1.20	2.45	2.73	0.70

Figure 2.7 shows the final position of the rocks in the FSI simulation for the 100-year flood event. Four rocks have moved in that simulation. Two of them: rock 25 (0.6 T) and rock 19 (0.8T) were moved away from the riprap installation. Rock 5 (1.0 T) and rock 37 (0.4 T) only moved locally. These results indicate that 1.0 T rocks in that installation are safe although they might be close to onset of motion. Smaller rocks may already move. Figure 2.7 additionally shows the trajectories of center of gravity for the moving rocks.

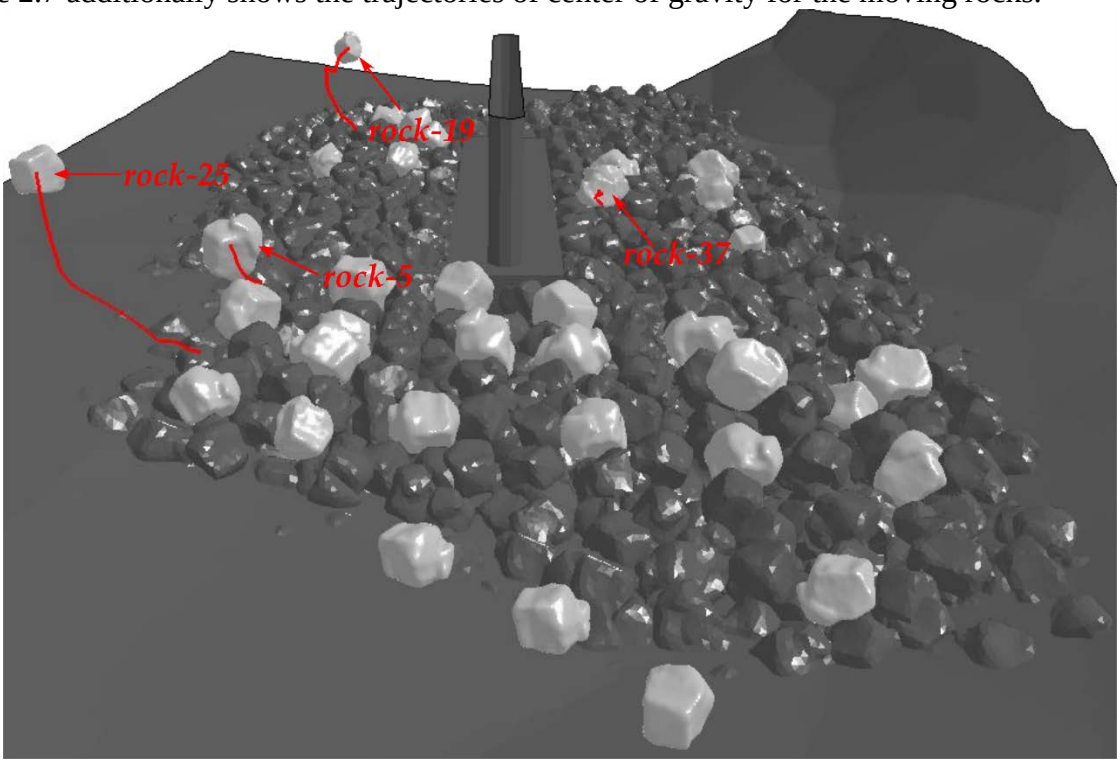

Figure 2.7: Initial trajectories of the moving rocks for the case Q100 discharge (11.1 ft/s average inlet velocity)

In order to verify at what conditions 1.0 T rocks start to move, several cases with higher inlet velocity into the scour subregion were considered. It has to be noted that, a scaled velocity on inlet faces by a factor of 1.5 for example does not correspond necessarily to specific conditions of 150-year flood in the river. Not only may the magnitude of the velocity change, but also the characteristics of the flow under the bridge might be slightly different in these conditions if the entire river is modeled. Overtopping of the road and the bridge may also occur for the larger floods and that would change the velocity profile around the bridge.

In one of the analyzed cases, the velocities on the inlet were multiplied by a factor of 1.2 (1.2 * Q100) to an average value of 4.1 m/s (13.3 ft/s). This case was only run to slightly above 1.0 sec of real time due to the problems with quickly changing mesh around interacting rocks. Table 2.2 shows maximum forces on three rocks within each weight group. For some of the rocks the ratio of the resultant force to their weight is very close to 1. That means if they are not blocked by other rocks around them, they will definitely be displaced from their initial positions. The FSI analysis indicates that nine rocks have moved. The simulation wasn't long enough to say for certain that more of them wouldn't move but within one second of simulated time they were not moving. Only one rock with a weight of one ton has moved, rock 5. Also only one rock with weight of 0.8 T, rock 19, was set in motion. Four rocks weighing 0.6 T have moved, rock 25, 26, 27, and 29. Two rocks weighing 0.4 T have moved, rock 35 and rock 37. Figure 2.8 shows the trajectories of center of gravity for the moving rocks.

Table 2.2: Forces on the critical rocks in the simulation with average inlet velocity 4.1 m/s (1.2 * Q100)

Rock #	X Force	Y Force	Z Force	Resultant	Ratio to weight
1 Ton (9.81 kN)					
6	-0.39	2.55	6.60	7.09	0.72
5	-1.11	3.41	5.57	6.62	0.68
8	-0.49	3.46	5.40	6.43	0.66
0.8 Ton (7.85 kN)					
19	-0.78	3.77	6.66	7.69	0.98
17	-0.36	2.41	3.81	4.52	0.58
13	0.29	1.51	4.03	4.31	0.55
0.6 Ton (5.88 kN)					
29	-0.58	1.66	4.36	4.70	0.80
25	-1.50	1.77	4.03	4.65	0.79
26	-0.46	1.34	4.37	4.59	0.78
0.4 ton (3.92 kN)					
35	0.55	1.70	3.64	4.05	1.03
39	-0.62	1.24	3.50	3.76	0.96
40	0.17	1.82	2.96	3.48	0.89

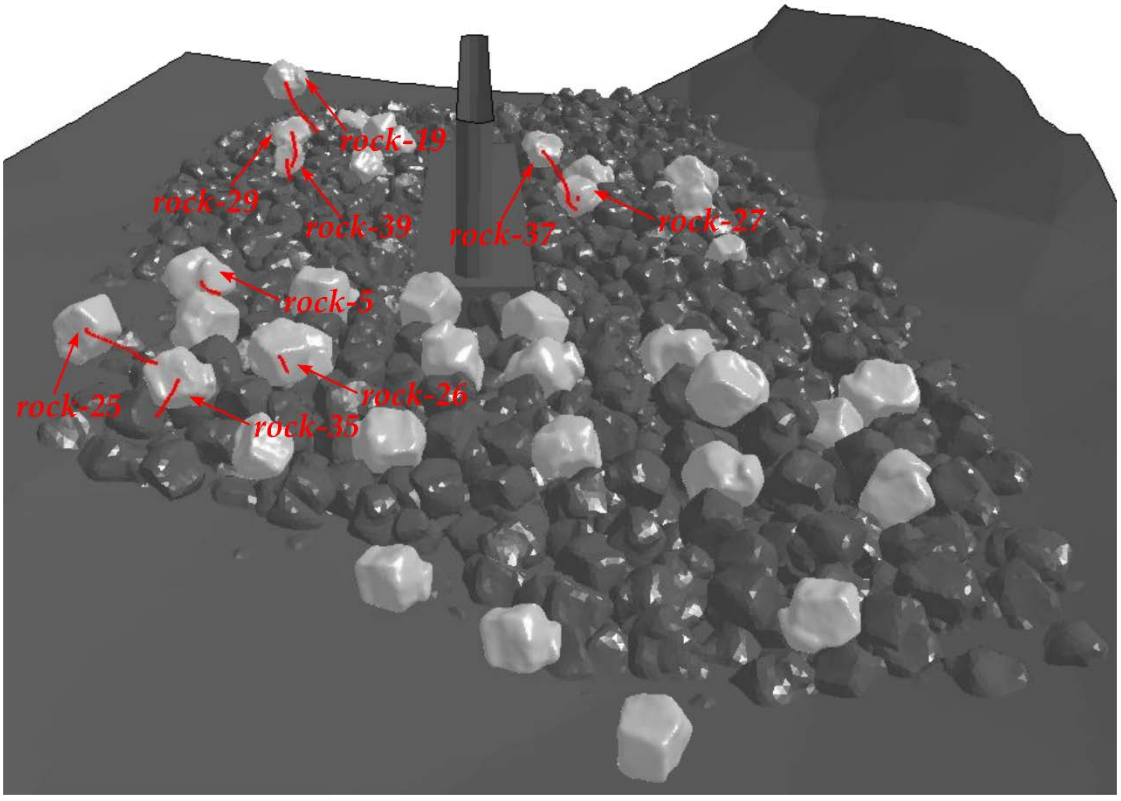

Figure 2.8: Initial trajectories of the moving rocks for the case 1.2 * Q100 discharge (4.1 m/s average inlet velocity)

Conclusions

A new advanced computational methodology for assessing failure risk of geometrically complex riprap installations or planned installations, including bridge support structure failure risk based on riprap size and shape, such as those found in field conditions has been developed.

This methodology solves the onset of motion analysis problem as a loosely coupled fluid structure interaction, FSI, problem. While using strong coupling and making all of the rocks in the riprap installation movable is conceptually possible and would be more accurate, that approach would be far too expensive and time consuming for reasonable engineering application to real field problems. As detailed in the paper, the explicit coupling is conservative and the procedure for assessing riprap failure risk and failure conditions for the specific geometry of a field riprap installation constitutes a major step forward in providing the capability to determine if an existing or planned riprap installation will be adequate.

The work included analysis of both a laboratory experiment where the onset of motion conditions was tested and result data was available (see report [2]), and an actual full-scale field case, the Middle Fork Feather River Bridge, which is located on State Route 89 in Plumas County, California near the town of Blairsden and Graeagle.

The modeling, analysis, and assessment of field sites, the Middle Fork Feather River Bridge case in this work, adds additional complexities that are often not present in well controlled laboratory experiments. Several observations can be made regarding field site conditions and the analysis results:

- A 3D scan of the riprap installation is useful in defining the boundaries of the riprap at the site but the data from the scan cannot be used directly in CAD software to generate the bed geometry of the computational domain because the scans do not capture hidden interstitial spaces between riprap rocks.
- Only a couple of the rocks were set in motion for the Q100 flood analysis, but that still indicates a condition that is on the verge of riprap failure.
- Analysis using Q100 flood velocity increased by 10% more than doubled the number of rocks set in motion to 5, and a case with velocity increased by 20% set eight rocks in motion, including 1 ton and smaller rocks. These results indicate that the current riprap size at the installation is close to minimum for stability of the installation in Q100 floods.
- The FSI analysis showed that onset of motion did not always occur for the rocks with the highest flow force to weight ratio. The reaction forces that arise from the arrangement and position of rocks with respect to their neighbors also plays a significant role in onset of motion. Therefore, the extent of interlocking in the arrangement and how well it constrains onset of motion, needs to be considered, as well as the flood flow velocity in the sizing of riprap.

The cost of applying the methodology is certainly much higher than a relatively quick calculation using any of the existing riprap sizing formulas, the amount of geometric detail and fundamental flow and rigid body physics applied in the new methodology is vastly greater. Therefore, good candidate applications for using FSI analysis to assess riprap installation would be those where the project cost is high, and therefore it is worth spending a fraction of the project funds to raise the confidence level that the riprap installation will keep the bridge foundations safe. New riprap projects or existing installations where the failure cost is much higher than the analysis cost are also good candidates for this type of advanced assessment methodology.

Acknowledgements

Argonne National Laboratory's work was supported by the U.S. Department of Transportation, Federal Highway Association, under interagency agreement with the U.S. Department of Energy under DE-AC02-06CH11357.

References

[1] U.S. Department of Transportation Federal Highway Administration, Bridge Scour and Stream Instability Countermeasures Experience, Selection, and Design Guidance Third Edition, Volume 1, NHI-09-111, 2009

[2] Bojanowski C., Lottes S., Development of a Computational Approach to Detect Instability and Incipient Motion of Large Riprap Rocks, Argonne National Laboratory, ANL/NE-17/14, August, 2017

[3] SIEMENS User Guide STAR-CCM+ Version 10.062, 2016.

[4] Hou G., Wang J., Layotn A., Numerical Methods for Fluid Structure Interaction – A Review, Commun. Comput. Phys., Vol. 12, No. 2, pp. 337-377, 2012.

[5] Livermore Software Technology Corporation (LSTC), LS-DYNA Keyword User's Manual Version 971, LSTC, 2016.

[6] Livermore Software Technology Corporation (LSTC), Incompressible fluid solver in LS-DYNA, LSTC, 2013.

[7] Flora K., Advanced Hydraulic Report for Pier Riprap Stability, Middle Fork Feather River Br. N. 09-0063, California Department of Transportation, June, 2014

[8] J. Sterling Jones Hydraulics Research Laboratory, https://www.fhwa.dot.gov/research/tfhrc/labs/hydraulics/ , Accessed: February 7, 2018.

[9] MeshLab, http://www.meshlab.net/ , Accessed: February 7, 2018

[10] Google Maps, Middle Fork Feather River, retrieved from: https://www.google.com/maps/place/Graeagle,+CA+96103/@39.7779978,-120.6238587,787m/data=!3m1!1e3!4m5!3m4!1s0x809c5c6208c3e323:0x9cdbe525708350e2!8m2!3d39.7662874!4d-120.6185519 , Accessed: April 16, 2018